Received: 22 September 2025 | Revised: 22 June 2026 | Accepted: 4 August 2026 | Published online: 3 September 2026

RESEARCH ARTICLE/REVIEW

Archives of Advanced Engineering Science
2026, Vol. 00(00) 1–16
DOI: 10.47852/bonviewAAES62027729

BON VIEW PUBLISHING

Enhanced Efficiency in Dual-Stage Grid-Connected Photovoltaic Systems with PSO-Integrated Hybrid MPPT Techniques

Yam Krishna Poudel[1,*], Jeewan Phuyal[1], Asmita Rijal[2] and Rashik Kumar Badgami[3]

[1] *Department of Electrical & Electronics, Nepal Engineering College, Pokhara University, Nepal*

[2] *Department of Hydro and Renewable Energy, Indian Institute of Technology (IIT), India*

[3] *Department of Artificial Intelligence, University of Cumberlands, USA*

Abstract: Maximum power point tracking (MPPT) is essential for maximizing photovoltaic (PV) energy conversion under variable irradiance and temperature. Conventional perturb and observe (P&O) and incremental conductance (INC) algorithms are simple to implement but may exhibit slow convergence, steady-state oscillations, and reduced tracking accuracy during rapid environmental changes. This study proposes two hybrid MPPT controllers—particle swarm optimization (PSO)-assisted P&O and PSO-assisted INC for a dual-stage grid-connected PV system. PSO adaptively determines the perturbation step size, while bounded duty-cycle constraints, transient PSO execution, and reduced perturbation near the maximum power point are applied to limit control jitter and improve stability. The proposed controllers were evaluated in MATLAB/Simulink under time-varying irradiance and temperature and compared with conventional P&O and INC methods. Both hybrid approaches improved power tracking, reduced oscillations at the DC–DC boost converter output, and maintained stable grid synchronization. The PSO–P&O controller achieved 97% efficiency, whereas PSO–INC reached 98.5%, demonstrating superior tracking accuracy and steady-state performance. These findings indicate that combining global PSO search with deterministic local tracking can enhance the efficiency, robustness, and reliability of grid-connected PV systems. Future work should validate the controllers experimentally under partial shading, grid disturbances, and real-time hardware conditions.

Keywords: particle swarm optimization, maximum power point tracking, incremental conductance, perturb and observe, grid-connected photovoltaic system

1. Introduction

Solar photovoltaic (PV) systems are increasingly being adopted in industrial and residential applications owing to their ability to significantly reduce greenhouse gas emissions. The clean energy produced by PV systems also powers automobiles, irrigation systems, satellites, and several other applications. However, factors such as solar radiation intensity and ambient temperature significantly influence the energy production efficiency of PV systems [1, 2]. Moreover, PV modules display considerable fluctuations in their current-voltage and power-voltage characteristics, demonstrating a nonlinear correlation [3]. This nonlinearity necessitates tuning to locate the maximum power point (MPP), where the system output is maximized. Optimization techniques such as perturb and observe (P&O) and incremental conductance (INC), which are easy to implement [4, 5], have been developed to maximize power extraction from PV systems by adjusting the voltage or duty cycle. Implementing maximum power point tracking (MPPT) methods in PV energy harvesters enhances the efficiency of energy collection, offering advantages such as the ability to reduce the size of solar panels and energy storage units [6].

Conventional optimization methodologies have distinct advantages and limitations in their implementation. The P&O method is known for its simplicity in tuning the MPP by periodically perturbing the PV voltage and observing the resulting output power. However, under steady-state conditions near the MPP, P&O may experience power losses owing to continuous perturbations [7]. Additionally, its performance can be limited by rapidly changing environmental conditions, such as fluctuations in irradiance or partial shading, which may cause it to lose track of the true MPP [8]. The INC method leverages the power derivative with respect to voltage to accurately locate the MPP by comparing the incremental and instantaneous conductances [9]. In general, especially in dynamic environments, INC algorithms suffer from increased computational complexity and the need for precise measurements, potentially leading to slower convergence and increased implementation costs [10].

Considering the limitations inherent in traditional MPPT techniques, researchers and engineers are actively developing

***Corresponding author:** Yam Krishna Poudel, Department of Electrical & Electronics, Nepal Engineering College, Pokhara University, Nepal. Email: yamkp@nec.edu.np

more robust approaches that demonstrate superior performance compared with conventional optimization methods. Advanced techniques such as particle swarm optimization (PSO), Artificial Neural Networks (ANNs), and Fuzzy Logic Control have been developed to enhance MPPT by improving accuracy and speed while reducing oscillations at the MPP [5, 11]. A key advantage of these approaches is their ability to identify the global optimum by generating random variables within the search space, thereby overcoming the limitations of traditional algorithms [12]. For instance, ANN-based MPPT controllers have recently gained prominence owing to their ability to predict the optimal operating point by learning from historical data, rendering them particularly suitable for environments with frequent variations [13]. In a study conducted by Ncir et al. [13], differential evolution in conjunction with a feedforward neural network was employed to achieve enhanced tracking speed and improved efficiency under various irradiance conditions. Hybrid methods that utilize PSO effectively address partial shading and the complex nonlinear traits of PV systems, thereby ensuring swift convergence to the global MPP [14]. These methods overcome the limitations of conventional techniques by dynamically adapting to real-time conditions, thereby improving their accuracy and reliability [14].

Hybrid MPPT techniques that integrate stochastic optimization methods with deterministic tracking algorithms have gained increasing attention due to their fast convergence and high tracking accuracy. However, such hybrid control schemes may encounter stability challenges, particularly in the form of duty-cycle oscillations and control jitter, when variable step-size perturbations are not properly regulated. Stochastic methods such as PSO introduce random exploration, while deterministic methods like P&O continuously adjust the operating point, which may lead to conflicting control actions near the MPP. Recent studies have investigated the stability of variable step-size MPPT algorithms and proposed damping and adaptive step-size mechanisms to mitigate oscillatory behavior and ensure smooth convergence [5, 15]. In this work, bounded duty-cycle limits, controlled PSO iteration phases, and reduced perturbation magnitudes are employed to enhance stability while preserving fast dynamic response.

In this research, the hybrid MPPT control technique is used, and the novelty lies in merging the PSO algorithm along with P&O first and then with INC algorithms. By performing this technique, the strengths of the particle and swarm method are integrated with the P&O method, due to which the overall performance of the system under the same input conditions can be enhanced, while also helping to mitigate their individual drawbacks under changing environmental conditions. Unlike many existing hybrid approaches that combine two or three algorithms without clearly defining their unique contributions, this approach aims to enhance tracking speed, accuracy, and stability by dynamically adjusting the control strategy based on real-time solar irradiance and temperature fluctuations, thus improving convergence to the global maximum power point (GMPP) [16]. This integration addresses the steady-state oscillations and slow response of P&O, the computational complexity of INC, and the local optima issues in traditional methods by using PSO's global search capability to optimize step sizes and control parameters adaptively [14]. The proposed method also includes a comparative evaluation under diverse environmental scenarios, demonstrating superior performance in efficiency and robustness compared to standalone and other hybrid MPPT techniques, which is often missing or insufficiently emphasized in prior studies [16]. By combining these algorithms in a novel control framework and validating it through simulation under realistic conditions, the study contributes a practical and effective solution for maximizing PV system energy output. This explicit focus on hybridizing PSO with both P&O and INC, along with detailed performance benchmarking, distinguishes the work from previous hybrid MPPT research that typically focuses on dual combinations or lacks comprehensive comparative analysis [17].

2. System Design

All the system design components are described as follows.

2.1. PV cell modeling

The equivalent circuit diagram of a PV system incorporates four parameters, which are a light-generated current (I_P), shunt resistance (R_{sh}), series resistance (R_{se}), and a diode (I_d). So, it is also known as four parameters model (Figure 1). The light-generated current varies with solar irradiance and cell temperature. Therefore, the relationship between the voltage and current of a PV cell can be expressed as follows [18].

Figure 1
Basic model of PV cell

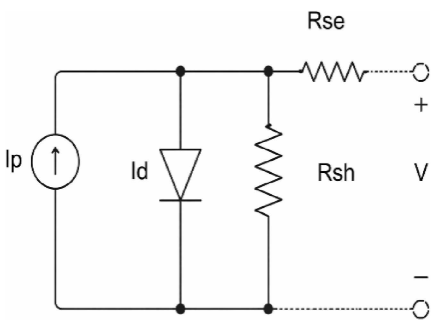

$$I = I_P - I_{rs}\left[\exp\left(\frac{q(V + IR_{se})}{\eta kT}\right) - 1\right] - \frac{V + IR_{se}}{R_{sh}} \quad (1)$$

In this context, I represents the output current of the solar cell, and V denotes its output voltage. The reverse saturation current of the diode is denoted by I_{rs} and equals 1.6×10^{-19} C. The deviation factor of the diode is represented by η, which is Boltzmann's constant (1.3807×10^{-23} JK^{-1}). T indicates the solar cell temperature, cell series, and shunt resistance. The P–V and I–C characteristics of the PV system are shown in Figure 2.

The electrical behavior of the solar cell was systematically characterized through its current–voltage (I–V) and power–voltage (P–V) profiles under three distinct irradiance levels: 0.6, 0.8, and 0.95 kW/m². The results reveal a pronounced current plateau across a broad voltage range, indicating stable charge carrier generation under illumination. However, as the terminal voltage approaches the threshold of approximately 35–40 V, a rapid decline in current is observed, marking the transition toward the open-circuit condition.

At the highest irradiance level of 0.95 kW/m², the solar cell exhibits a peak current close to 9 A, reflecting the strong dependence of photocurrent on incident solar intensity. This behavior underscores the direct proportionality between irradiance and

Figure 2
I–V and P–V characteristics of solar cell

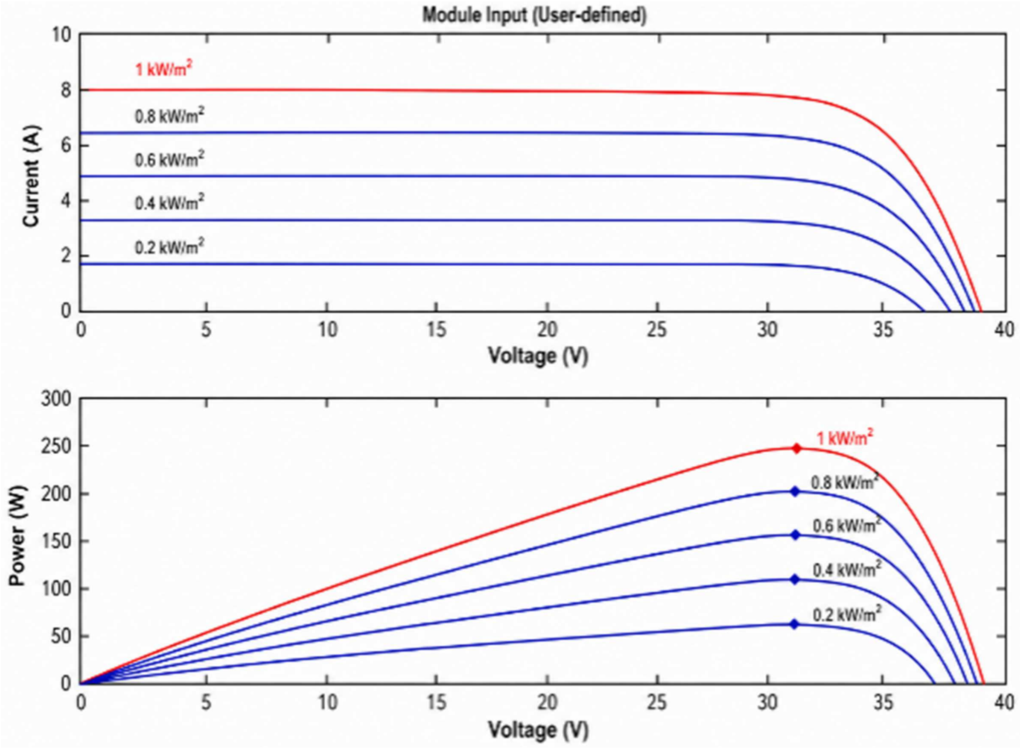

current generation, while also highlighting the inherent nonlinearity of the I–V characteristic near the voltage limit (Figure 2)

This analysis demonstrates that higher irradiance enhances solar cell performance by increasing both current and power output. The I–V and P–V curves provide essential insight into the cell's operational behavior and efficiency under varying solar conditions.

2.2. DC–DC boost converter

A DC–DC converter converts a fixed direct current (DC) voltage to a variable DC voltage. While performing the MPPT algorithm, the power that is obtained from the PV module is analyzed, and necessary adjustments are made by incrementing or decrementing the voltage and current values so that maximum output power can be achieved. In order to convert the input DC voltage to the required steady output voltage as per requirement, the values of duty cycle (D) are adjusted between zero and one, which eventually results in achieving the required DC output voltage [19].

$$V_o = V_s/(1 - D) \tag{2}$$

where V_o refers to the output voltage of the boost converter, V_s is the source voltage, and D is the duty ratio. As illustrated in Figure 3, a boost converter requires several components: a DC input voltage source, an inductor, a switch (typically an IGBT), a diode, a capacitive filter, and a load. The duty ratio can be adjusted to modify the output voltage. In order to maintain the continuous conduction mode, it is essential to determine the critical inductance and capacitance, which ensure an uninterrupted current flow through the load.

Figure 3
Basic schematic of DC–DC boost converter

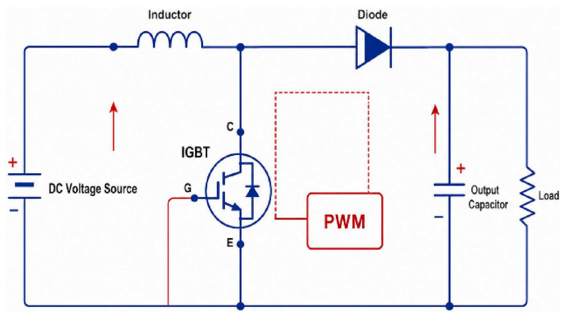

$$L_c = \frac{D(1 - D)^2 \times R}{2f} \tag{3}$$

$$C_c = \frac{D}{2fR} \tag{4}$$

The value of critical inductance helps to determine for which time the load current remains uninterrupted and can conduct continuously; it means that for the continuous conduction of the current toward the load, the value of the inductor in the converter must be higher than the value of critical inductance, and it is represented as L_c.

Similarly, the critical capacitance (C_c) value represents the value of the capacitor for which it can maintain the continuous capacitor voltage. It suggests achieving the desired performance; the value of capacitance must be greater than the critical value in this converter.

2.3. Dual-stage grid-connected PV system

The output of the PV module cannot be directly interfaced with the utility grid under all operating conditions. Before grid connection, criteria such as phase sequence, voltage, and frequency matching must be satisfied. A dual-stage grid-connected PV system includes a DC-to-DC converter followed by a DC-to-alternating current (AC) converter to produce high-quality AC power suitable for grid synchronization (Figure 4). In this process, first, the obtained DC power is passed through a boost converter to obtain appropriate voltage, which is maintained by a DC link capacitor, as DC-link capacitors help protect the circuit from voltage spikes and electromagnetic interference (EMI), and it is placed mostly between the DC-to-DC converter circuit and inverter circuit.

The three-phase inverter serves as the interface that transforms DC power into AC, enabling seamless interaction with the grid. To enhance power quality, an output filter composed of inductors L_1, L_2, and capacitor C is employed, effectively smoothing the waveform and mitigating harmonics.

The control architecture is designed with a high level of sophistication, integrating multiple coordinated subsystems. A pulse-width modulation (PWM) generator governs the inverter switching, while a phase-locked loop (P_{ll}) ensures precise synchronization with the grid. Transformations between the abc and dq reference frames enable efficient control in a rotating coordinate system, and cascaded control loops with proportional–integral (PI) regulators maintain system stability and dynamic performance.

Real-time measurements of current and voltage I_{abc} & V_{abc} are continuously fed back into the control system, allowing adaptive regulation and reliable grid integration. In the outer control loop, a single PI controller is utilized to regulate the DC-link voltage, ensuring it accurately tracks the reference value $V_{dc,ref}$ and maintains overall system balance.

Concurrently, internal loop current regulation employs a pair of controllers to manage the direct and quadrature currents. The overall relationship between the grid-connected inverter voltages and line currents is as follows [20]:

$$[e_a e_b e_c] = R_f [I_a I_b I_c] + L_f \, d/dt \, [I_a I_b I_c] + [V_a V_b V_c] \quad (5)$$

where e_a, e_b, and e_c represent the inverter output voltages; I_a, I_b and I_c denote the three-phase line currents; V_a, V_b, and V_c correspond to the three-phase grid voltages; and R_f and L_f are the filter resistance and inductance, respectively.

In order to transform three-phase electrical parameters into dq-axis components, Park's transformation technique is used, due to which grid synchronization becomes possible with the PV system.

This process incorporates a phase-locked loop (PLL) based on the synchronous reference frame. The mathematical representation of the reference frame that rotates in sync with the voltage of the grid can be expressed as follows [20, 21]:

$$V_d = e_d - R_f I_d + \omega L_f - L(dI_d)/dt \quad (6)$$

$$V_q = e_q - R_f I_q + \omega L_f I_d - L\left(dI_q\right)/dt \quad (7)$$

Figure 4
Dual-stage grid-connected PV system control scheme

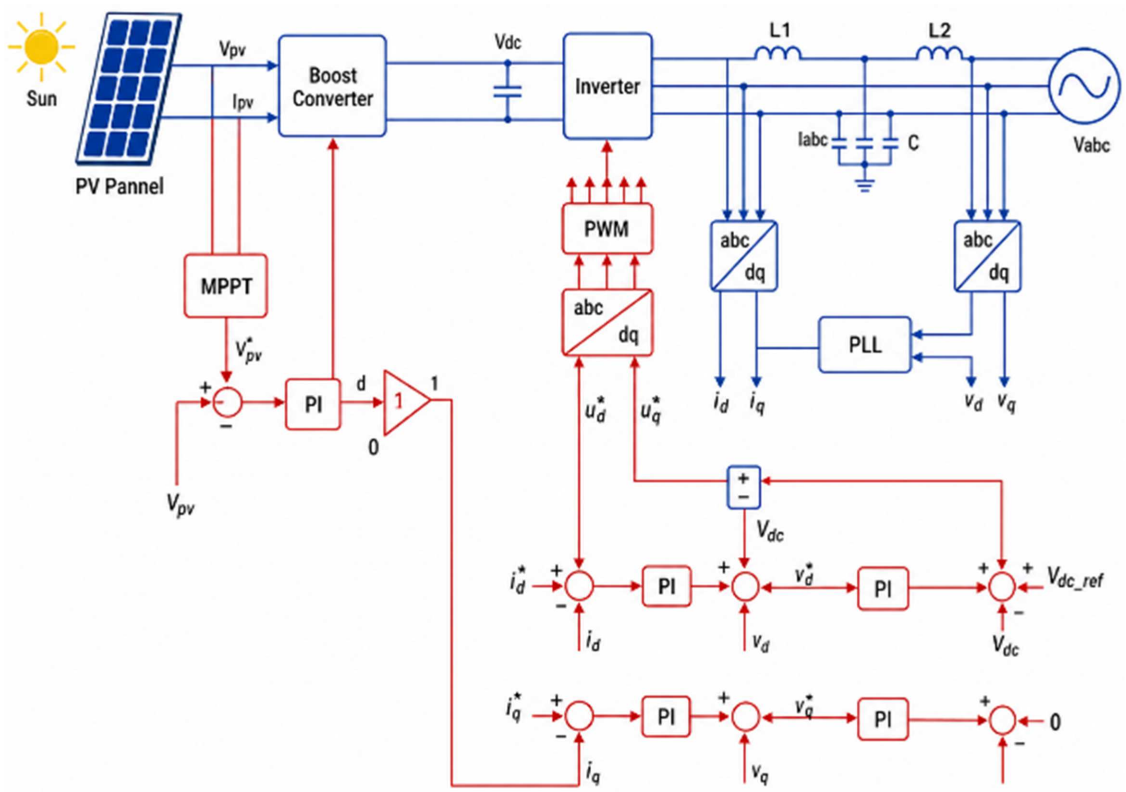

where V_d and V_q are the grid d-axis and q-axis voltage components, respectively; e_d and e_q are the d-axis and q-axis inverter voltage components, respectively; I_d and I_q are the d-axis and q-axis grid currents, respectively; and ω is the angular frequency [21].

2.4. System specifications and configuration

In this research method, the required parameters of the PV module, PSO algorithm, boost converter, and grid-tied PV system are tabulated below (Table 1). Regarding the parameters used in the PV module, it includes the open-circuit voltage (V_oc), short-circuit current (I_sc), and maximum power specifications for a particular value of irradiance and temperature, which is 1000 W/m^2 and 25 °C.

In addition, optimization of the power output requires parameter initialization like inertia weight (w), cognitive coefficient (C_1), and social coefficient (C_2), which are very essential in the PSO algorithm. Furthermore, in a boost converter, the values of resistances, inductance, capacitance, and other filter components decide the performance of the DC-to-DC conversion, so that the required performance can be achieved. Lastly, the parameters for the grid-tied PV array, which incorporate the filter capacitance, filter inductance, grid frequency, grid voltage, and switching frequency of the inverter, help to ensure optimal energy conversion and integration to the grid and provide a solid structure for performance analysis.

3. MPP and Optimization Algorithms

The MPP of a PV system is defined as the operational state at which the PV system achieves its optimal efficiency, yielding the maximum attainable power output [22]. As previously discussed, various optimization techniques, including P&O and INC, are frequently utilized to achieve the maximum power output in PV systems. These conventional techniques are not only straightforward to implement but also serve as references and benchmarks for newly developed hybrid and advanced MPPT techniques [5]. This section briefly discusses the proposed P&O-, INC-, and PSO-based models for the optimal power extraction from PV systems.

3.1. Perturb and observe (P&O)

P&O is a widely used optimization technique for extracting optimum power from PV systems. This approach involves

Table 1
Parameters settings for the study

Parameter	Value
PV module (1000 W/m², 25 °C)	
Open-circuit voltage (Voc)	38.4 V (grid-tied: 36.3 V)
Short-circuit current (Isc)	8.85 A (grid-tied: 7.35 A)
Maximum power	248.977 W (grid-tied: 213.15 W)
Voltage at maximum power point	30.7 V (grid-tied: 29 V)
Current at maximum power point	8.11 A (grid-tied: 7.35 A)
Parallel strings	1 (grid-tied: 8)
Series modules per string	1 (grid-tied: 25)
PV system capacity	40 kW
PSO algorithm	
Inertia weight (w)	1
Cognitive coefficient (c_1)	1.5
Social coefficient (c_2)	1.5
Boost converter	
Input capacitance (C_i)	100 µF
Input resistance (R_i)	0.0001 Ω
Inductance in inductive filter (L)	2 mH
Resistance in inductive filter (R)	0.1 Ω
Capacitance in capacitive filter (C_i)	100 µF
Resistance in capacitive filter (R)	0.0001 Ω
Load resistance (R)	20 Ω
Grid-tied PV array simulation	
Filter capacitance (Cfilter)	20 µF
Filter inductance (Lfilter)	20 µF
Inductance in inductive filter (L)	7 mH
Grid voltage (VLL)	400 V
Grid frequency (f)	50 Hz
Inverter switching frequency (fsw)	10 kHz

making minor adjustments to the operating voltage while concurrently monitoring the resulting changes in the power output to determine the MPP [7, 23]. If the power increases subsequent to a change in voltage, the adjustment is iterated until the maximum power is attained, with the power calculated through the measurement of voltage and current, and the differentials from the previous values evaluated [23]. At the MPP, the change in power is zero; otherwise, the algorithm adjusts the voltage using a fixed step size, shifting the operating point as required to approach the MPP. This continuous adjustment enhances energy collection while maintaining a balance between the tracking speed and stability, despite potential fluctuations [24]. This method alters the duty cycle of the converter, which induces a perturbation in the system voltage [25]. Choosing the appropriate perturbation step size and sampling rate is essential because a smaller step size ensures stability but slows down tracking, whereas a larger step size accelerates tracking at the risk of increased fluctuations [26]. Figure 5 [14, 28] depicts the basic flow of the conventional P&O algorithm. In PV system, the output power is given as $P = V \times I$, where V is the voltage and I is the current. The P&O algorithm disturbs the voltage and observes the resulting change in power. If $\Delta P/\Delta V > 0$, then the voltage is increased. If $\Delta P/\Delta V < 0$, the voltage decreases, and the changes are repeated until the system converges at the MPP, where $\Delta P/\Delta V = 0$.

Figure 5
Conventional perturb and observe algorithm

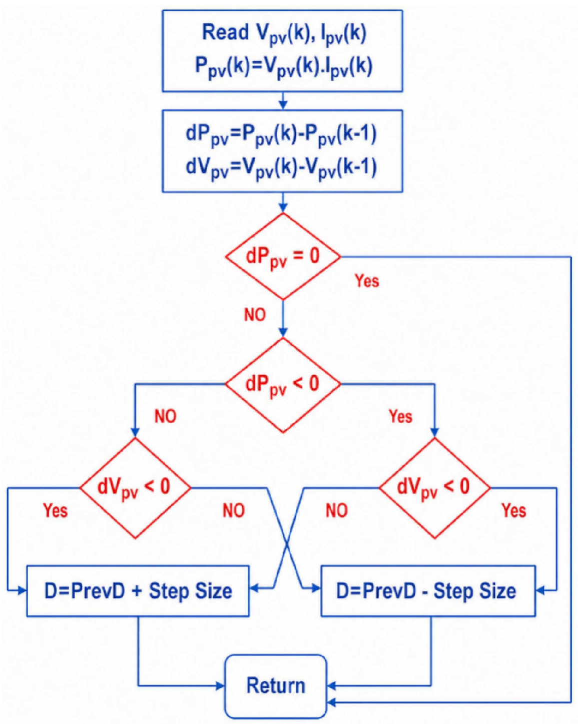

Researchers have demonstrated the efficacy of the P&O method in real-world applications for high MPPT [23]. Studies have demonstrated the satisfactory efficiency of the P&O method, citing its effective energy collection from PV panels [23]. Nevertheless, this methodology has been criticized for its propensity to induce oscillations around the MPP, potentially resulting in energy inefficiencies, particularly under dynamic environmental conditions or partial shading scenarios [8]. Moreover, slow convergence speed with steady-state oscillations, drift under sudden irradiance variation, difficulty in recognizing the global MPP under partially shaded conditions, and becoming trapped in the local MPP are significant challenges [8, 27]. Despite certain limitations, P&O has contributed significantly to various innovations in controlling techniques for efficient MPP tracking under diverse conditions.

3.2. Incremental conductance (INC)

Another widely used technique for optimizing PV systems to achieve maximum power is the INC algorithm. This technique evaluates the differential conductance (dI/dV) and contrasts it with the instantaneous conductance (I/V) [4]. When dI/dV is equal to $-I/V$, the system reaches the MPP [29]. The INC algorithm can determine whether the MPP has been achieved by computing the incremental changes in the current and voltage. The operating point is adjusted based on the slope of the PV power curve [29]. Researchers have noted that INC is generally more accurate than P&O, with better performance under fluctuating weather conditions [10]. In contrast to P&O, which depends on disturbances, INC utilizes the connection between differential conductance (dI/dV) and immediate conductance (I/V) [9].

The INC method determines the MPP by utilizing the principle that the derivative of power with respect to voltage (dP/dV) equals zero at the MPP [29]. This can be mathematically represented as $dI/dV = -I/V$, where I is the current and V is the voltage. In this method, the algorithm continuously measures the voltage and current from the solar panel, calculating the changes in voltage (ΔV) and current (ΔI). It then evaluates the ratio of $\Delta I/\Delta V$. When $\Delta I/\Delta V = -I/V$, the system is at the MPP. If $\Delta I/\Delta V > -I/V$, the voltage is adjusted upward, while if $\Delta I/\Delta V < -I/V$, the voltage adjusted downward, enabling the system to track the MPP effectively under varying environmental conditions. This methodology accurately tracks the MPP under rapidly changing conditions, ensuring efficient operation without the oscillations observed in alternative methods, such as P&O [9]. INC effectively maximizes energy harvesting from solar panels [21]. Critics contend that implementing INC presents greater challenges than simpler methods, such as P&O [10]. The approach to the MPP can be impeded when the voltage deviates significantly from the optimal value or when subjected to rapid fluctuations in irradiance [29]. Similar to P&O, this method exhibits poor convergence speed and accuracy [21]. Notwithstanding these inherent challenges, the INC method remains an efficacious approach for optimizing power extraction from PV systems, thereby establishing itself as a reliable MPPT method [9, 28]. Figure 6 [14, 28] illustrates the basic flowchart for INC optimization.

3.3. Particle swarm optimization (PSO)

PSO is an algorithm that emulates the collective movement of bird flocks and fish schools using a population-based approach (Figure 7) [14, 30, 33]. PSO aims to identify optimal or near-optimal solutions to complex problems through an iterative process that refines potential solutions based on specific measures of quality or fitness [30]. In PSO, a collection of candidate solutions, known as particles, explores the problem space to identify the optimal solution [30]. Each particle updates its position based on its own experience and that of its neighbors, gradually converging toward the optimal solution identified by the swarm [31]. Each particle serves as a candidate solution to the optimization problem and is characterized by its specific position and velocity

Figure 6
The conventional incremental conductance algorithms

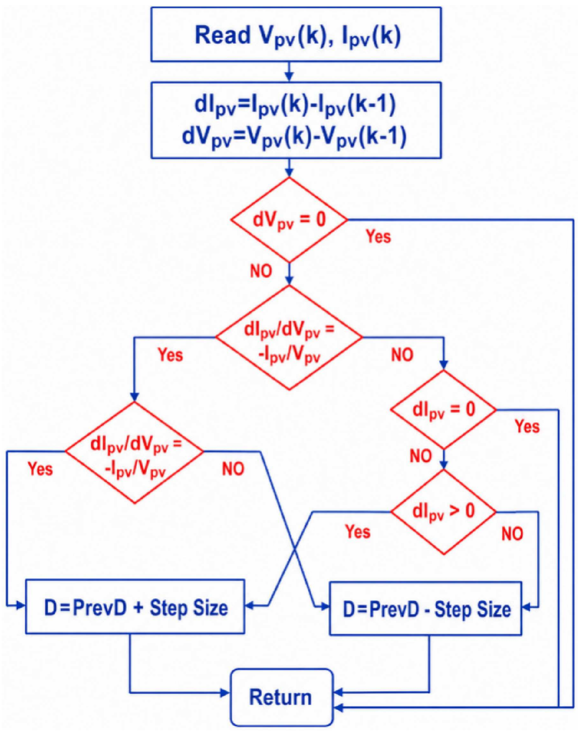

Figure 7
Flowchart of PSO

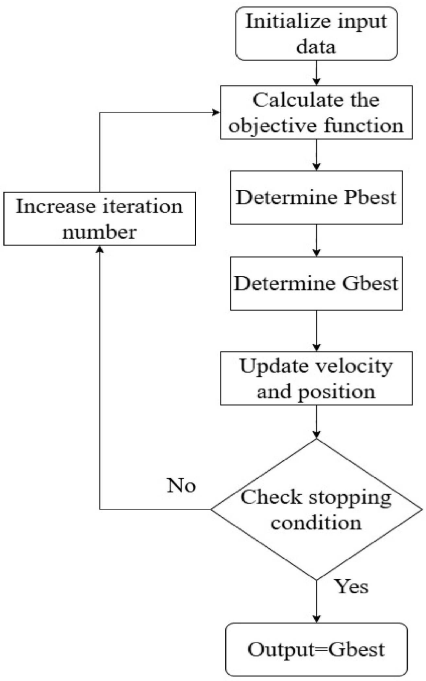

within the search domain [32]. The motion of each particle is influenced by its personal best position (Pbest) and the best positions identified by its neighboring particles (global best or Gbest), where Pbest represents the optimal position attained by a particle in its history and Gbest denotes the optimal position discovered by any particle within the entire swarm [32]. The velocity and position of each particle are updated using the following equations [31].

$$V_i(t+1) = W \times V_i(t) + c_1 \times r\_1[(Pbest)\_(i) - X_i(t)] + c_2 \times r_2[(Gbest)\_ - X\_i(t)] \quad (8)$$

$$X_i(t+1) = X_i(t) + V_i(t+1) \quad (9)$$

Here, V_i(t) and X_i(t) are the velocity and position of particle i at time t, W is the inertia weight, c_1 and c_2 are acceleration coefficients, and r_1 and r_2 are random numbers between 0 and 1.

Researchers have increasingly utilized PSO to achieve MPPT in PV systems and have demonstrated its superior performance in tracking GMPPs compared to traditional techniques [33, 34]. However, researchers have described several limitations of PSO-based MPPT methods, such as long convergence times and oscillations during the search process [33, 35]. Researchers have proposed modifications or innovative methods to address these disadvantages, including hybrid methods combined with traditional methods [34].

3.4. Proposed PSO-based MPPT optimization

A previous study indicated that hybrid optimization techniques are advantageous for maximizing the efficiency of PV systems. We integrated PSO with conventional methodologies in our model to increase the output power and improve the convergence speed to expedite the MPP identification. In addition, the hybrid PSO and P&O optimization method reduces the possibility of converging to the local minima in comparison to traditional methods, which results in reduced oscillations around the MPP. The strength of this proposed hybrid model is that the perturbation step size is dynamically adjusted using a swarm intelligence approach, and it results in an enhanced convergence rate and reduced oscillations around the MPP.

Furthermore, the PSO and INC hybrid model helps to accurately track maximum power under dynamic environmental conditions such as partial shading and highly dynamic irradiance conditions. The main focus in this paper is to improve the efficiency, accuracy, and reliability of the solar PV systems and maximize the energy using the PSO + P&O and PSO + INC approaches.

The particles represent different perturbation steps in the PSO-based P&O method. The position and velocity were enhanced using the PSO algorithm. The position and velocity updates are as follows [31]:

$$X_i(t+1) = X_i(t) + V_i(t+1) \quad (10)$$

$$V_i(t+1) = W \cdot V_i(t) + c_1 \cdot r_1 \cdot (P_i best - X_i(t)) + c_2 \cdot r_2(Gbest - X_i(t)) \quad (11)$$

where X_i represents the position of the particle i, V_i represents velocity, w is the inertia weight, c_1 and c_2 are cognitive and social coefficients, r_1 and r_2 are random numbers, P_i *best* is the best-known position of particle i, and *Gbest* is the global best position. Similarly, the conductance calculations in the PSO + INC method are similar but optimized using PSO with position and velocity updates. These enhancements enable both techniques to dynamically adjust their search for the MPP, thereby significantly improving their efficiency and adaptability to changing environmental conditions. A flowchart of the PSO-based hybrid optimization is presented in Figure 8.

Figure 8
Flowchart of proposed PSO-driven P&O/INC optimization

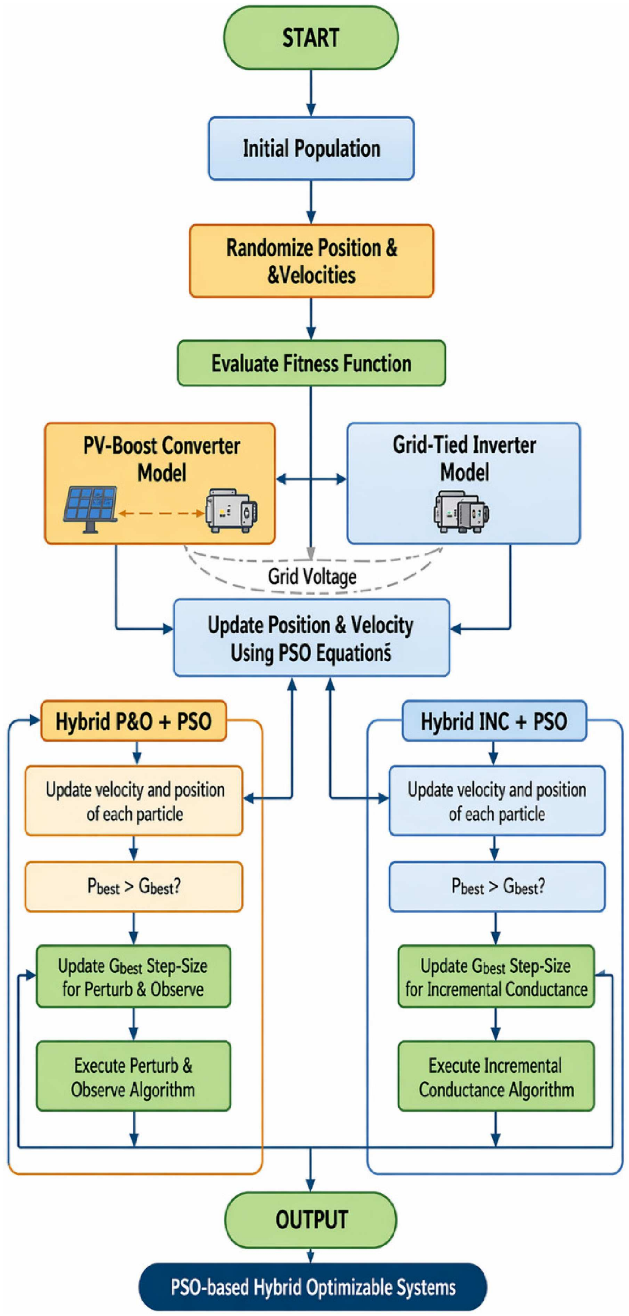

4. Simulations and Result

A comprehensive Simulink model (Figure 9) was developed to represent a solar energy conversion system integrated with advanced power optimization control. The system is initiated by a PV module interfaced with a DC–DC boost converter, comprising key components such as an IGBT switch, diode, and inductor to facilitate efficient voltage stepping and energy transfer. The control framework incorporates a PWM scheme to regulate the switching dynamics of the converter, ensuring optimal power extraction. Distributed measurement and monitoring blocks are embedded throughout the model to continuously track critical parameters, including voltage, current, and power. Furthermore, the system is governed by closed-loop feedback mechanisms and intelligent control algorithms that implement MPPT strategies, thereby enhancing overall energy efficiency. Visualization tools, including scopes and display blocks, are integrated to enable real-time observation of system performance and output responses. This model serves as a robust platform for simulating and analyzing the dynamic behavior of a solar power conversion system, along with its associated control architecture under varying operating conditions.

The Simulink model depicts a grid-connected PV system. The simulation model commenced with a PV array (represented by a solar panel icon) that generated DC power from solar energy (Figure 10). The system includes power conditioning stages, most notably a three-phase inverter that converts the DC power from the PV array into three-phase AC power suitable for grid integration. The inverter section contains multiple IGBT/diode pairs controlled by PWM signals for appropriate power conversion. A three-phase distribution grid connection incorporates appropriate inductors (*L1*, *L2*, and *L3*) for filtering and synchronizing the grid. The upper section of the diagram illustrates the control system components, including the PWM generation and various measurement blocks for monitoring the system parameters. This setup represents a typical grid-tied solar power system that enables renewable energy to be fed into the utility grid while maintaining proper power quality and grid synchronization requirements.

The hybrid MPPT algorithm integrates PSO for global peak detection with INC for high-precision local tracking. During the initial global search phase, a swarm of 100 particles explores the duty-cycle step-size space $\Delta D \in [0, 0.5]$ over 100 iterations, utilizing an inertia weight $w = 1$ and acceleration coefficients $c_1 = c_2 = 1.5$ to converge upon the GMPP. Once the optimal step size is identified (gbest), the system transitions to the INC phase, which regulates the duty cycle D within a [0, 0.8] range by comparing the instantaneous conductance I/V against the INC $\Delta I/\Delta V$. While this dual-stage approach effectively minimizes steady-state oscillations, its reliance on a simplified power model and the absence of a dedicated shading detection trigger suggest that performance may vary under complex partial shading scenarios.

In this control system, a three-phase inverter is designed using a direct–quadrature (dq) frame transformation technique, as illustrated in Figure 11. Overall, this system is divided into two main parts, where the first left-side part is the PLL using DQ frame transformation so that sine-cosine reference signals can be generated, while the right-side part consists of a three-phase current controller of the inverter using DQ transformation. Functionally, the PLL section is responsible for synchronization with the grid frequency, and the current controller part is responsible for the regulation of the inverter output. This complete control architecture is very crucial for a grid-tied inverter system as it enables proper synchronization with the grid along with accurate current control in a rotating reference frame, which makes the control system highly stable and efficient in order to get the desired result. Block PI controllers and feedback loops help to monitor and maintain stable operation along with the quality of power of the grid-connected inverters.

The performance of PV systems is contingent on solar irradiance and temperature, which are critical parameters. Solar irradiance, ambient temperature, and relative humidity significantly influence PV power output under various climatic conditions [36]. In general, higher temperatures negatively impact PV panel efficiency. In our model, the dynamic response of the PV system to short-term environmental variations specifically irradiance and temperature over a 10 s interval was systematically simulated. Solar irradiance, expressed in W/m², represents

Figure 9
The Simulink model of the PV system implemented algorithms and a boost converter

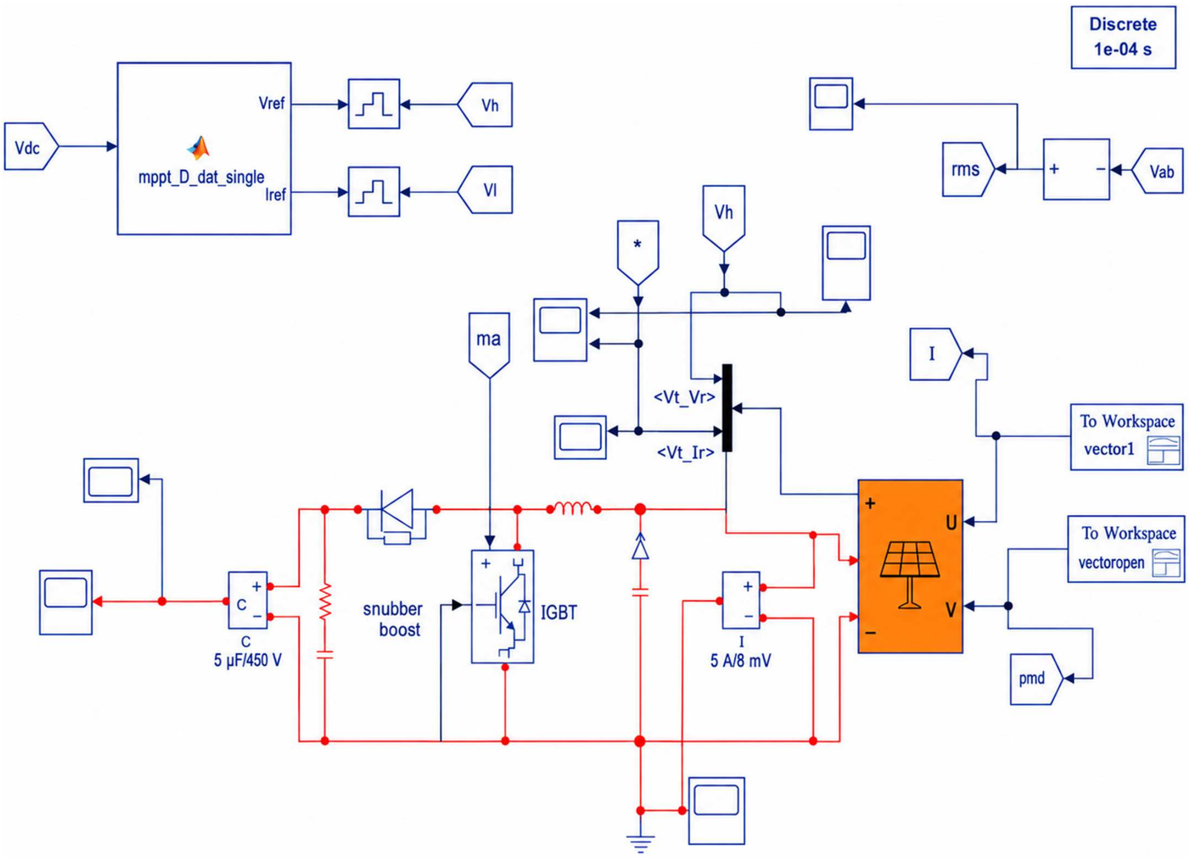

Figure 10
Grid-connected PV systems

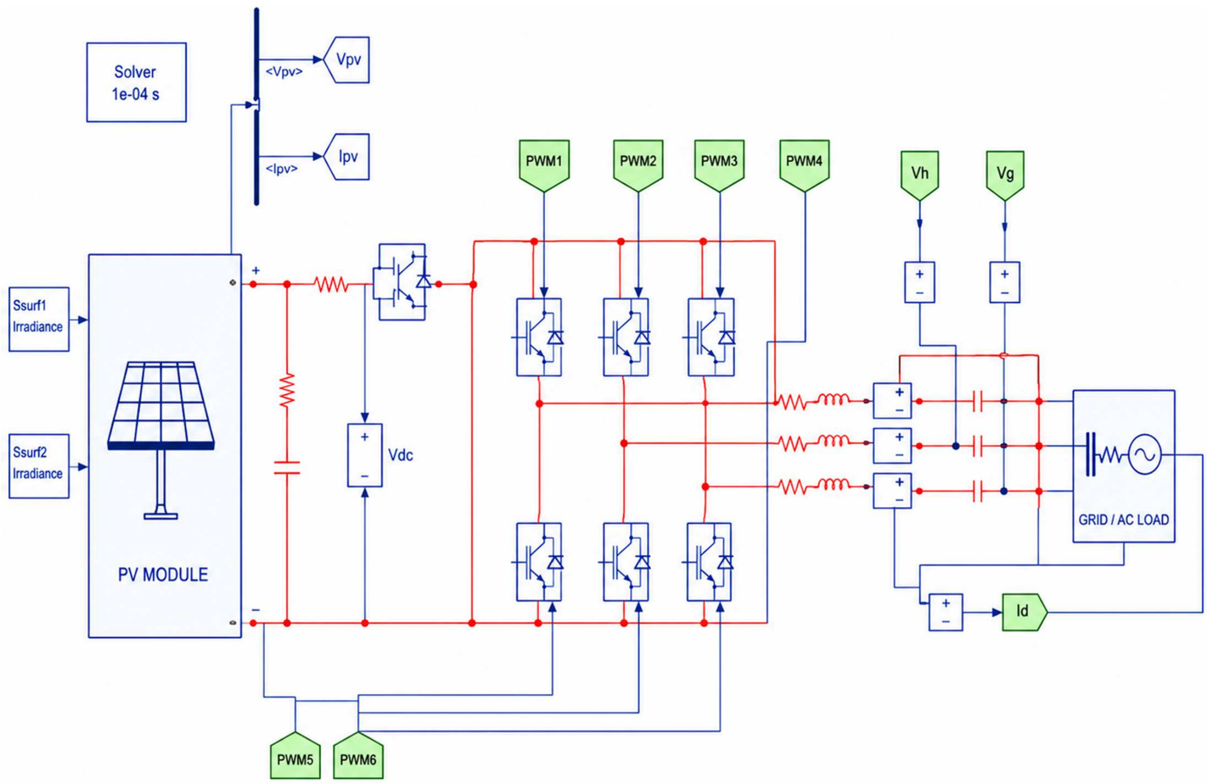

Figure 11
Control structure of grid

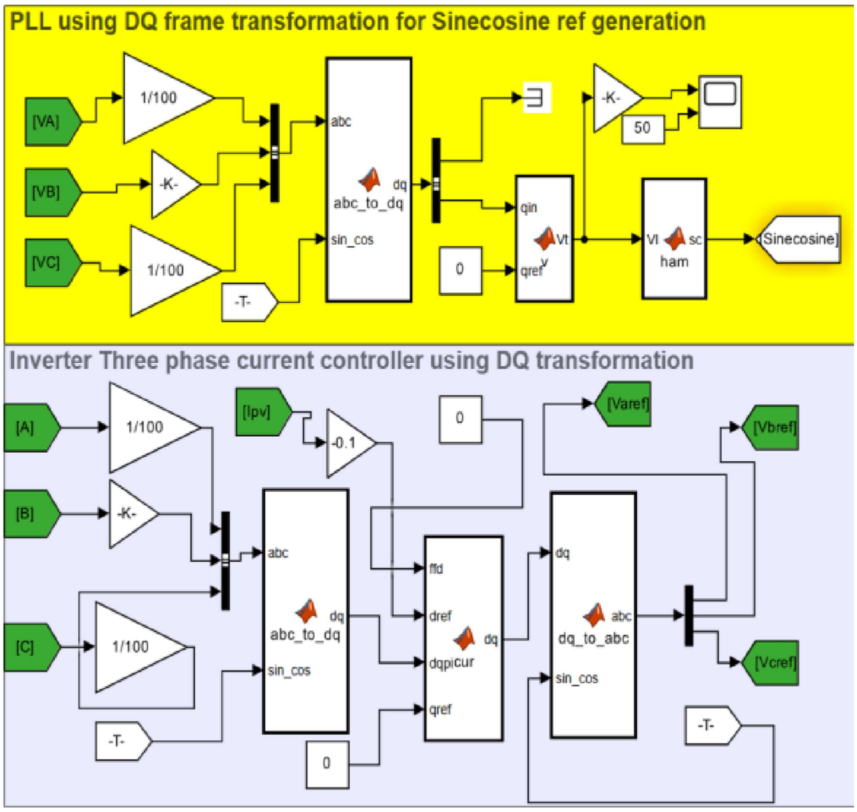

Figure 12
Input (a) irradiance and (b) temperature

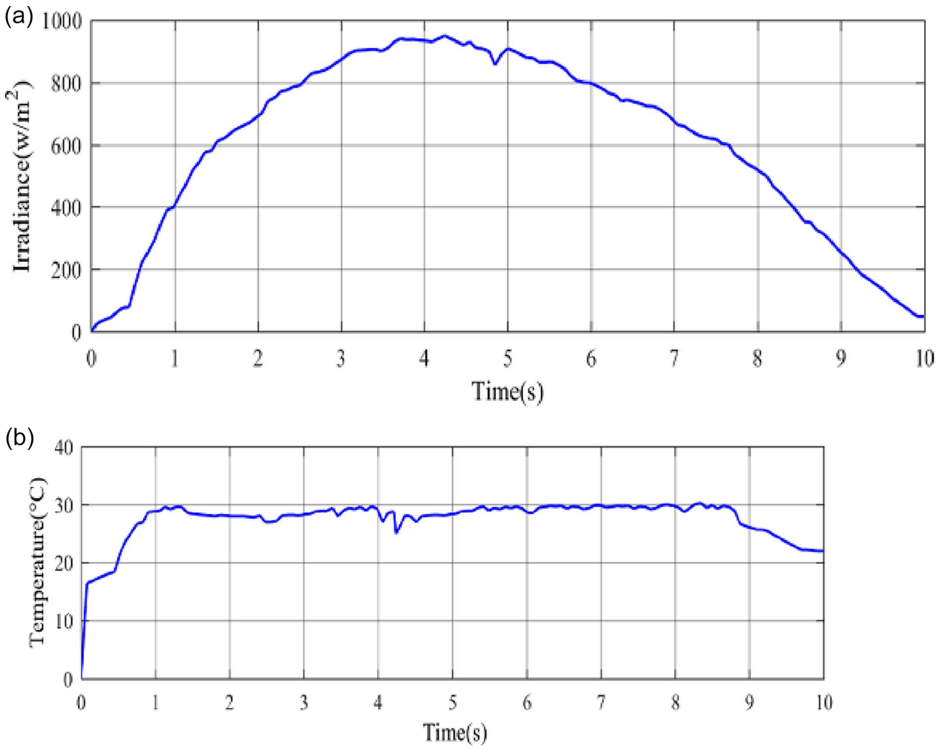

the incident solar energy on the PV surface (Figure 12(a)). The irradiance profile follows a Gaussian distribution, initiating at zero, reaching a peak value of approximately 900 W/m² around 4–5 s, and subsequently declining to zero by the end of the simulation. This behavior effectively emulates transient atmospheric conditions such as passing cloud cover and fluctuating solar exposure. Figure 12(b) illustrates the temperature profile (°C), corresponding to the operating temperature of the PV module. The temperature begins at approximately 10 °C, rises rapidly to around 25–30 °C within the first second, and thereafter remains relatively stable with minor fluctuations for the duration of the simulation.

In our simulation without MPPT, we analyzed the power output and efficiency of a dual-stage grid-connected PV system and observed a significant discrepancy between the ideal and actual power. Although the ideal curve peaked at 220 W, the actual PV output remained at approximately 60 W, indicating substantial power loss and inefficient energy harvesting (Figure 13(a)). The efficiency reached over 90% but could not be maintained over the period, dropping to 30% during the middle period, which demonstrates the importance of the MPPT controller (Figure 13(b)). With the implementation of the P&O MPPT controller, the PV system demonstrated notable improvements in power and efficiency. The PV output power closely followed the ideal power curve, reaching approximately 200–220 W (Figure 13(c)). Similarly, the system exhibited a substantially stable efficiency, averaging 90–95% throughout most of the operating period (Figure 13(d)). The boost converter power

Figure 13
System response without MPPT: (a) PV output power and (b) PV system efficiency; system response with P&O MPPT: (c) PV output power, (d) PV system efficiency, and (e) boost converter power; system response with incremental conductance MPPT: (f) PV output power, (g) PV system efficiency, and (h) boost converter power, respectively

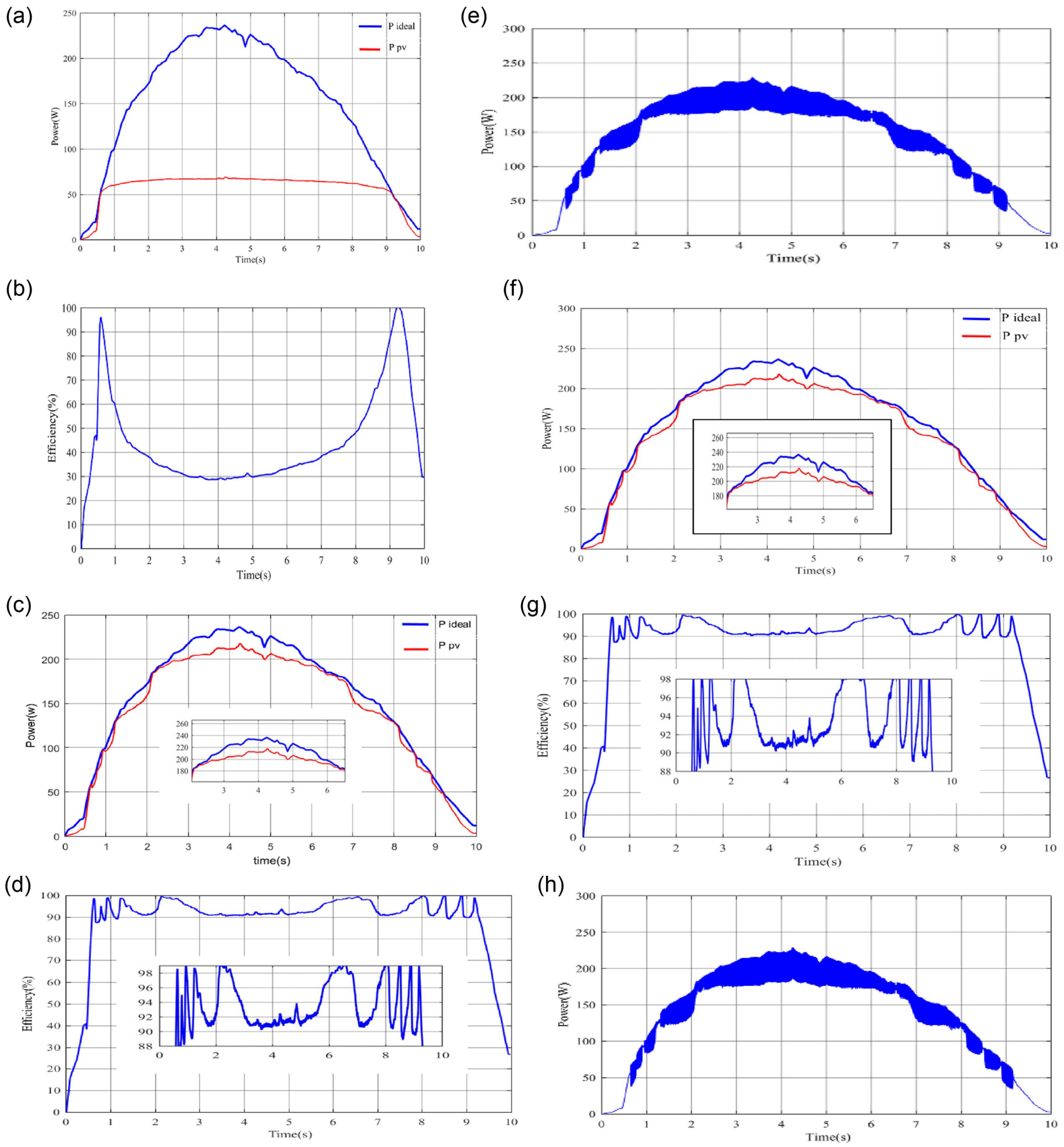

Figure 14
Power-tracking, efficiency, and boost converter performance of hybrid P&O–PSO and INC–PSO MPPT controllers under varying irradiance conditions

(a)
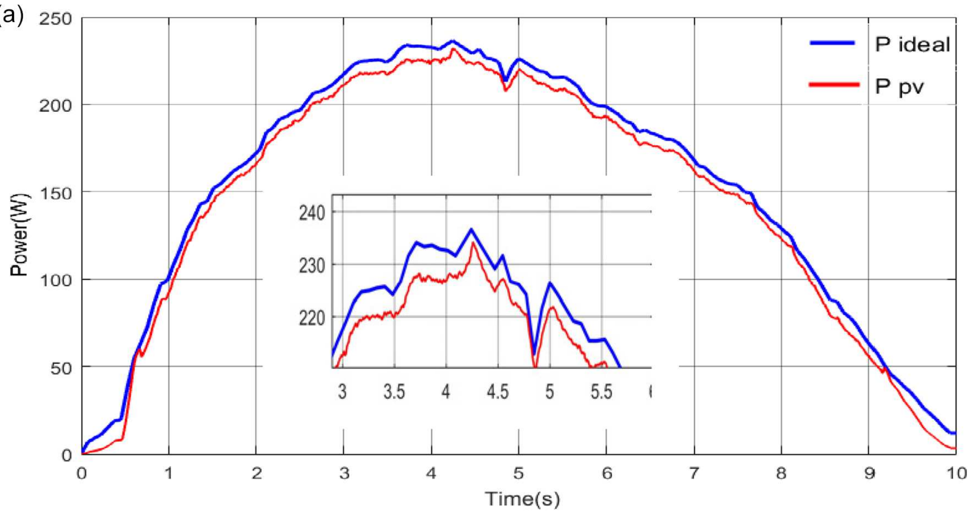

(b)
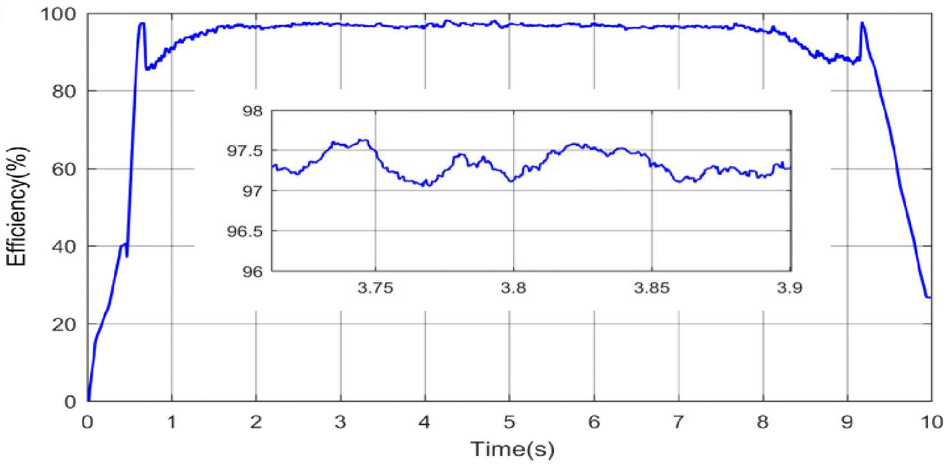

(c)
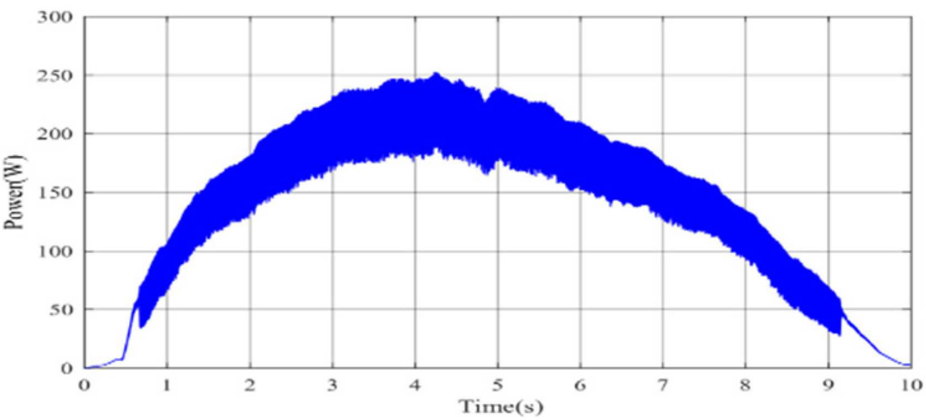

Figure 14
(*continued*)

(d)
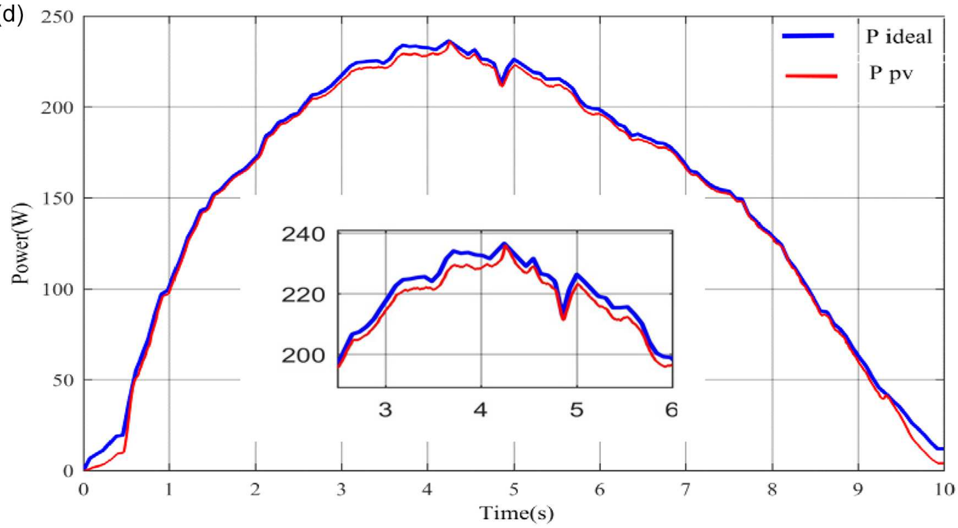

(e)
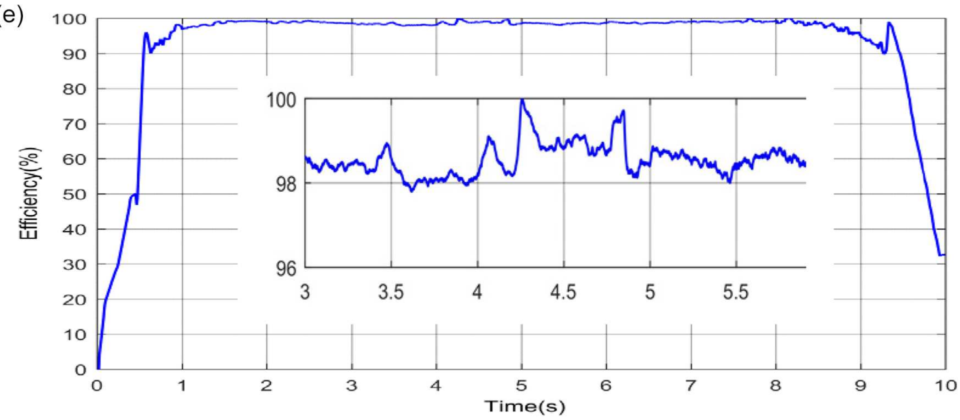

(f)
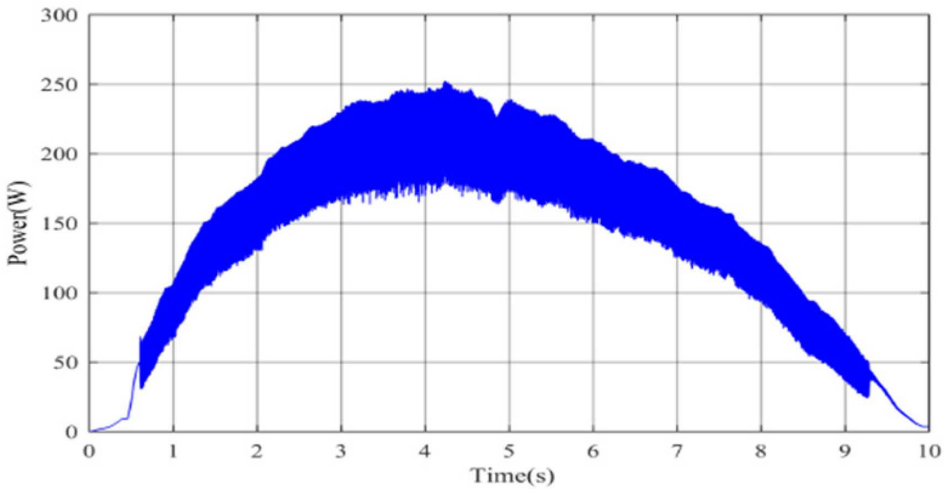

Figure 15
Output grid current, voltage and frequency

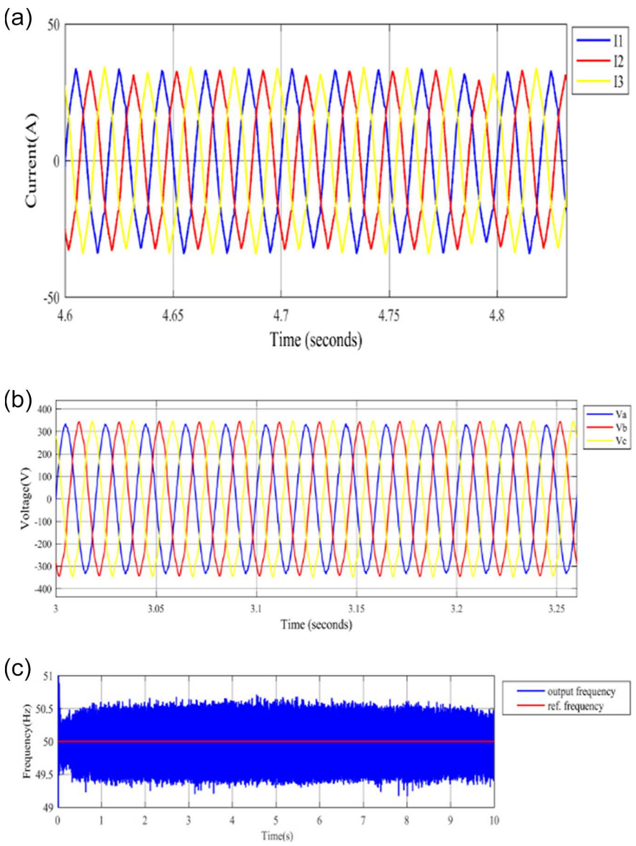

output closely resembles a smooth bell curve over time, indicating effective power conversion and delivery to the load (Figure 13(e)). Similarly, the performance of the INC MPPT controller was comparable to that of the P&O controller. However, it exhibited slightly more pronounced oscillations in tracking the ideal power curve (Figure 13(f)) and efficiency (Figure 13(g)) while having a similar pattern with more pronounced fluctuations compared to the P&O method (Figure 13(h)). The boost converter power output remained virtually identical between the two methods. Overall, we observed improvements in the power and efficiency curves for both MPPT controllers, with the P&O controller offering marginally more stable operation with fewer oscillations.

We employed hybrid approaches (P&O + PSO and INC + PSO) and observed that they exhibited notable improvements over their traditional counterparts. Both hybrid controllers demonstrated superior power-tracking capabilities with reduced oscillations around the MPP (Figures 14(a) and (d)). The efficiency of the systems for both models maintained consistently high levels of approximately 95%, with INC + PSO exhibiting slightly more stable efficiency than P&O + PSO (Figures 14(b) and (e)). The power output from the boost converter in the hybrid models displayed reduced oscillations with a smoother output curve compared to the traditional P&O and INC methods (Figures 14(c) and (f)). In this study, we successfully integrated a double-stage grid-tied PV system with synchronous parameters. The three-phase current and voltage waveforms exhibited proper synchronization with a stable grid frequency, indicating effective operation with improved MPPT control (Figure 15(a)-(c)). Overall, the hybridization of PSO with P&O and INC led to further improvements, with PSO + INC demonstrating superior efficiency (Table 2). A comparison revealed that PSO integration functioned more effectively with INC than with P&O integration. In addition, the PV system (P&O MPPT) was successfully synchronized with the grid at a voltage of approximately 380 V and a frequency close to 50 Hz, indicating effective grid integration under varying irradiance conditions.

Figure 14 presents the dynamic performance of the system under hybrid MPPT strategies. For the hybrid P&O + PSO approach, subfigures (a), (b), and (c) illustrate the PV output power, PV system efficiency, and boost converter power, respectively. Similarly, for the hybrid INC + PSO approach, subfigures (d), (e), and (f) depict the corresponding PV output power, PV system efficiency, and boost converter power, providing a comprehensive comparison of system behavior under both optimization techniques.

Figure 15 illustrates the dynamic response of the grid-tied PV system under MPPT operation, depicting (a) the synchronized grid current, (b) the synchronized grid voltage, and (c) the synchronized grid frequency.

5. Conclusions and Recommendations

MPPT plays a pivotal role in maximizing the energy output of PV systems, especially in environments subject to unpredictable variations in sunlight intensity and temperature. This research presents a robust hybrid framework that integrates PSO with the established P&O and INC algorithms. The innovative dual-stage grid-connected architecture leverages PSO's global search capabilities to circumvent local maxima pitfalls, which is a common limitation in purely deterministic MPPT methods. Concurrently, it utilizes INC and P&O for fine-tuned local optimization, enhancing the system's accuracy in locating the MPP. Simulation results indicate that the proposed hybrid configurations significantly outperform traditional deterministic approaches. Specifically, the PSO+INC configuration achieved an outstanding tracking efficiency of 98.5%. This level of efficiency not only optimizes power extraction but also addresses the inherent trade-offs between convergence speed and steady-state oscillations, which often hinder system performance and energy yield. To further bolster system stability and reliability, a dq-frame transformation current controller was implemented,

Table 2
Comparison of MPPT optimization efficiency

MPPT algorithm	Step size	Efficiency (η) %
P&O	0.0005	95%
INC	0.0005	95%
PSO + P&O	0–0.5	97%
PSO + INC	0–0.5	98.5%

ensuring effective synchronization with the power grid. This controller maintains stable frequency and voltage profiles even in fluctuating irradiance conditions, a crucial requirement for the reliable operation of grid-connected PV systems. Despite these advancements in efficiency and stability, the study acknowledges certain limitations. The dependence on a simplified power model could introduce performance variability, particularly in extreme situations involving non-uniform partial shading conditions, where light intensity discrepancies across the solar panel can occur. Future research is directed toward two key areas: (i) conducting comprehensive experimental validations in real-world, large-scale dual-stage grid-connected networks to evaluate the system's robustness against grid transients and environmental fluctuations and (ii) investigating advanced artificial intelligence techniques to enhance adaptive control strategies under conditions of high uncertainty. In summary, the hybridization of PSO with the INC method presents a promising and effective approach for integrating modern renewable energy systems, significantly enhancing the potential for maximizing energy harvesting and improving the performance of PV technologies under variable environmental conditions.

Acknowledgment

The authors are grateful to RSD Kaushalam Pvt. Ltd. for the assistance in data analysis in the high-performance computer lab.

Ethical Statement

This study does not contain any studies with human or animal subjects performed by any of the authors.

Conflicts of Interest

The authors declare that they have no conflicts of interest to this work.

Data Availability Statement

Data are available from the corresponding author upon reasonable request.

Declaration of Generative AI and AI-Assisted Technologies in the Writing Process

During the preparation of this study, tools such as Grammarly and PaperPal were used for grammar and formatting checks. The authors subsequently reviewed and refined the manuscript and take full responsibility for its content.

Author Contribution Statement

Yam Krishna Poudel: Methodology, Software, Validation, Formal analysis, Investigation, Resources, Data curation, Writing - original draft, Writing - review & editing, Visualization, Supervision, Project administration. **Jeewan Phuyal:** Formal analysis, Investigation, Data curation, Writing - review & editing, Visualization, Project administration. **Asmita Rijal:** Investigation, Resources. **Rashik Kumar Badgami:** Software, Resources.

References

[1] Gao, Y., Chen, B., Wu, D., Dai, Z., Wang, C., & Zhang, X. (2022). Comparative study of various solar power generation systems integrated with nanofluid-flat heat pipe. *Applied Energy*, *327*, 120052. https://doi.org/10.1016/j.apenergy.2022.120052

[2] Han, Z., Liu, K., Li, G., Zhao, X., & Shittu, S. (2021). Electrical and thermal performance comparison between PVT-ST and PV-ST systems. *Energy*, *237*, 121589. https://doi.org/10.1016/j.energy.2021.121589

[3] Mannino, G., Tina, G. M., Jiménez-Castillo, G., Cacciato, M., Bizzarri, F., & Canino, A. (2024). Nonlinear and multivariate regression models of current and voltage at maximum power point of bifacial photovoltaic strings. *Solar Energy*, *269*, 112357. https://doi.org/10.1016/j.solener.2024.112357

[4] Ishaque, K., Salam, Z., & Lauss, G. (2014). The performance of perturb and observe and incremental conductance maximum power point tracking method under dynamic weather conditions. *Applied Energy*, *119*, 228–236. https://doi.org/10.1016/j.apenergy.2013.12.054

[5] Abidi, H., Sidhom, L., & Chihi, I. (2023). Systematic literature review and benchmarking for photovoltaic MPPT techniques. *Energies*, *16*(8), 3509. https://doi.org/10.3390/en16083509

[6] Brunelli, D., Dondi, D., Bertacchini, A., Larcher, L., Pavan, P., & Benini, L. (2009). Photovoltaic scavenging systems: Modeling and optimization. *Microelectronics Journal*, *40*(9), 1337–1344. https://doi.org/10.1016/j.mejo.2008.08.013

[7] Saberi, A., Niroomand, M., & Dehkordi, B. M. (2023). An improved P&O based MPPT for PV systems with reduced steady-state oscillation. *International Journal of Energy Research*, *2023*(1), 4694583. https://doi.org/10.1155/2023/4694583

[8] Jabbar, R. I., Mohammed, K. K., Mekhilef, S., Mubin, M., Seyedmahmoudian, M., Stojcevski, A., . . . , & Becherif, M. (2023). A modified P&O-MPPT technique using fuzzy logic controller for PV systems. In *2023 IEEE IAS Global Conference on Emerging Technologies (GlobConET)*, 1–7. https://doi.org/10.1109/GlobConET56651.2023.10149991

[9] Shang, L., Guo, H., & Zhu, W. (2020). An improved MPPT control strategy based on incremental conductance algorithm. *Protection and Control of Modern Power Systems*, *5*(1), 14. https://doi.org/10.1186/s41601-020-00161-z

[10] Chellakhi, A., El Beid, S., Abouelmahjoub, Y., & Doubabi, H. (2024). An enhanced incremental conductance MPPT approach for PV power optimization: A simulation and experimental study. *Arabian Journal for Science and Engineering*, *49*(12), 16045–16064. https://doi.org/10.1007/s13369-024-08804-1

[11] Tariq, M., Rihan, M., & Ayan, M. (2024). A comprehensive review on the application of recently introduced optimization techniques obtaining maximum power in the solar PV System. *Renewable Energy Focus*, *49*, 100564. https://doi.org/10.1016/j.ref.2024.100564

[12] Rezk, H., Fathy, A., & Abdelaziz, A. Y. (2017). A comparison of different global MPPT techniques based on meta-heuristic algorithms for photovoltaic system subjected to partial shading conditions. *Renewable and Sustainable Energy Reviews*, *74*, 377–386. https://doi.org/10.1016/j.rser.2017.02.051

[13] Ncir, N., El Akchioui, N., & El Fathi, A. (2023). Enhancing photovoltaic system modeling and control under partial and

complex shading conditions using a robust hybrid DE-FFNN MPPT strategy. *Renewable Energy Focus*, *47*, 100504. https://doi.org/10.1016/j.ref.2023.100504
[14] Ibrahim, M. H., Ang, S. P., Dani, M. N., Rahman, M. I., Petra, R., & Sulthan, S. M. (2023). Optimizing step-size of perturb & observe and incremental conductance MPPT techniques using PSO for grid-tied PV system. *IEEE Access*, *11*, 13079–13090. https://doi.org/10.1109/ACCESS.2023.3242979
[15] Djilali, A. B., Bounadja, E., Yahdou, A., Benbouhenni, H., Elbarbary, Z. M. S., Colak, I., & Al-Gahtani, S. F. (2025). Enhanced variable step sizes perturb and observe MPPT control to reduce energy loss in photovoltaic systems. *Scientific Reports*, *15*(1), 11700. https://doi.org/10.1038/s41598-025-95309-y
[16] Abbas, A., Farhan, M., Shahzad, M., Liaqat, R., & Ijaz, U. (2025). Power tracking and performance analysis of hybrid perturb–observe, particle swarm optimization, and fuzzy logic-based improved MPPT control for standalone PV system. *Technologies*, *13*(3), 112. https://doi.org/10.3390/technologies13030112
[17] Melhaoui, M., Rhiat, M., Oukili, M., Atmane, I., Hirech, K., Bossoufi, B., . . . , & Alenezi, M. (2025). Hybrid fuzzy logic approach for enhanced MPPT control in PV systems. *Scientific Reports*, *15*(1), 19235. https://doi.org/10.1038/s41598-025-03154-w
[18] Quaschning, V., & Hanitsch, R. (1996). Numerical simulation of current-voltage characteristics of photovoltaic systems with shaded solar cells. *Solar Energy*, *56*(6), 513–520. https://doi.org/10.1016/0038-092X(96)00006-0
[19] Nakpin, A., & Khwan-on, S. (2016). A novel high step-up DC-DC converter for photovoltaic applications. *Procedia Computer Science*, *86*, 409–412. https://doi.org/10.1016/j.procs.2016.05.051
[20] Lakshmanan, S. A., Jain, A., & Rajpourhit, B. S. (2014). A novel current controlled technique with feed forward DC voltage regulator for grid connected solar PV system. In *2014 Eighteenth National Power Systems Conference (NPSC)*, 1–6. https://doi.org/10.1109/NPSC.2014.7103892
[21] Shengqing, L., Fujun, L., Jian, Z., Wen, C., & Donghui, Z. (2020). An improved MPPT control strategy based on incremental conductance method. *Soft Computing*, *24*(8), 6039–6046. https://doi.org/10.1007/s00500-020-04723-z
[22] Eltamaly, A. M. (2021). Photovoltaic maximum power point trackers: An overview. In S. Motahhir & A. M. Eltamaly (Eds.), *Advanced technologies for solar photovoltaics energy systems* (pp. 117–200). Springer International Publishing. https://doi.org/10.1007/978-3-030-64565-6_6
[23] Kacimi, N., Idir, A., Grouni, S., & Boucherit, M. S. (2022). Improved MPPT control strategy for PV connected to grid using IncCond-PSO-MPC approach. *CSEE Journal of Power and Energy Systems*, *9*(3), 1008–1020. https://doi.org/10.17775/CSEEJPES.2021.08810
[24] Owusu-Nyarko, I., Elgenedy, M. A., Abdelsalam, I., & Ahmed, K. H. (2021). Modified variable step-size incremental conductance MPPT technique for photovoltaic systems. *Electronics*, *10*(19), 2331. https://doi.org/10.3390/electronics10192331
[25] Femia, N., Petrone, G., Spagnuolo, G., & Vitelli, M. (2004). Optimizing duty-cycle perturbation of P&O MPPT technique. *2004 IEEE 35th Annual Power Electronics Specialists Conference (IEEE Cat. No. 04CH37551)*, *3*, 1939–1944. https://doi.org/10.1109/PESC.2004.1355414
[26] Yan, K., Du, Y., & Ren, Z. (2018). MPPT perturbation optimization of photovoltaic power systems based on solar irradiance data classification. *IEEE Transactions on Sustainable Energy*, *10*(2), 514–521. https://doi.org/10.1109/TSTE.2018.2834415
[27] Sundareswaran, K., Vigneshkumar, V., Sankar, P., Simon, S. P., Nayak, P. S. R., & Palani, S. (2015). Development of an improved P&O algorithm assisted through a colony of foraging ants for MPPT in PV system. *IEEE Transactions on Industrial Informatics*, *12*(1), 187–200. https://doi.org/10.1109/TII.2015.2502428
[28] Putri, R. I., Wibowo, S., & Rifa'i, M. (2015). Maximum power point tracking for photovoltaic using incremental conductance method. *Energy Procedia*, *68*, 22–30. https://doi.org/10.1016/j.egypro.2015.03.228
[29] Liu, Y. H., Chen, G. J., Liu, C. L., & Su, C. Y. (2024). Comprehensive review on fast maximum power point tracking algorithms for solar power generation systems. *Ain Shams Engineering Journal*, *15*(12), 103093. https://doi.org/10.1016/j.asej.2024.103093
[30] Gad, A. G. (2022). Particle swarm optimization algorithm and its applications: A systematic review: AG gad. *Archives of Computational Methods in Engineering*, *29*(5), 2531–2561. https://doi.org/10.1007/s11831-021-09694-4
[31] Shami, T. M., Mirjalili, S., Al-Eryani, Y., Daoudi, K., Izadi, S., & Abualigah, L. (2023). Velocity pausing particle swarm optimization: A novel variant for global optimization. *Neural Computing and Applications*, *35*(12), 9193–9223. https://doi.org/10.1007/s00521-022-08179-0
[32] Li, Y., Zhang, Y., & Hu, W. (2023). Adaptive multi-objective particle swarm optimization based on virtual Pareto front. *Information Sciences*, *625*, 206–236. https://doi.org/10.1016/j.ins.2022.12.079
[33] Alshareef, M., Lin, Z., Ma, M., & Cao, W. (2019). Accelerated particle swarm optimization for photovoltaic maximum power point tracking under partial shading conditions. *Energies*, *12*(4), 623. https://doi.org/10.3390/en12040623
[34] Lian, K. L., Jhang, J. H., & Tian, I. S. (2014). A maximum power point tracking method based on perturb-and-observe combined with particle swarm optimization. *IEEE Journal of Photovoltaics*, *4*(2), 626–633. https://doi.org/10.1109/JPHOTOV.2013.2297513
[35] Koh, J. S., Tan, R. H., Lim, W. H., & Tan, N. M. (2023). A modified particle swarm optimization for efficient maximum power point tracking under partial shading condition. *IEEE Transactions on Sustainable Energy*, *14*(3), 1822–1834. https://doi.org/10.1109/TSTE.2023.3250710
[36] Hassan, M. A., Bailek, N., Bouchouicha, K., Ibrahim, A., Jamil, B., Kuriqi, A., . . . , & El-kenawy, E. S. M. (2022). Evaluation of energy extraction of PV systems affected by environmental factors under real outdoor conditions. *Theoretical and Applied Climatology*, *150*(1), 715–729. https://doi.org/10.1007/s00704-022-04166-6

How to Cite: Poudel, Y. K., Phuyal, J., Rijal, A., & Badgami, R. K. (2026). Enhanced Efficiency in Dual-Stage Grid-Connected Photovoltaic Systems with PSO-Integrated Hybrid MPPT Techniques. *Archives of Advanced Engineering Science*. https://doi.org/10.47852/bonviewAAES62027729